Progress in Nuclear Energy 101 (2017) 288–298

Contents lists available at ScienceDirect

Progress in Nuclear Energy

journal homepage: www.elsevier.com/locate/pnucene

Sensitivity of power spectral density techniques to numerical parameters in analyzing neutron noise experiments

E. Gilad [a, *], B. Geslot [b], P. Blaise [b], C. Dubi [c]

[a] The Unit of Nuclear Engineering, Ben-Gurion University of the Negev, Beer-Sheva 84105, Israel
[b] DEN/CAD/DER/SPEx/LPE, CEA Cadarache, Saint-Paul-les-Durance 13108, France
[c] Department of Physics, Nuclear Research Center NEGEV (NRCN), Beer-Sheva 84190, Israel

ARTICLE INFO

Article history:
Received 15 September 2016
Received in revised form
7 January 2017
Accepted 21 March 2017
Available online 2 April 2017

Keywords:
Noise techniques
Power spectral density
Sensitivity analysis
Integral kinetic parameters
Spectrum calculations

ABSTRACT

Power spectral density (PSD) methods are well-known and widely used for the analysis of neutron noise experiments and obtaining the reactor's integral kinetic parameters, i.e., the effective delayed neutron fraction β_{eff} and the prompt neutron generation time Λ. Many uncertainties are usually associated with PSD methods, e.g., statistical fluctuations in the neutron flux, power drifts, uncertainties in the Diven factor, the integral fission rate, and in the reactivity value. However, the uncertainty associated with the numerical parameters used in the power spectrum calculation procedure is hardly discussed in the literature and generally overlooked.

The aim of this paper is to study the uncertainties in the kinetic parameters of a reactor core, obtained by PSD methods, which are associated with the numerical parameters of the method. A comprehensive estimation of the kinetic parameters, including all other uncertainties, is not pursued. In this paper, PSD methods are implemented to analyze critical and subcritical configurations of the MINERVE zero power reactor in order to measure its integral kinetic parameters β_{eff} and Λ. Both cross and auto power spectral densities are calculated and the kinetic parameters are obtained via Lorentzian curve fitting over the calculated PSD. The sensitivity of the obtained kinetic parameters to the choice of numerical parameters used for spectrum calculations is studied and found to be significant with respect to other uncertainties. A novel methodology is proposed for analyzing the kinetic parameters' sensitivity to the PSD calculations and for quantifying the associated uncertainties.

1. Introduction

A set of neutron noise measurements has been performed on the MINERVE zero power reactor at Cadarache research center in France during September 2014. This experimental campaign was conducted in the framework of a tri-partite collaboration between CEA, PSI and SCK-CEN (Geslot et al., 2015; Perret, 2015; Gilad et al., 2016). Measurements were then also processed and analyzed in the framework of a collaboration between CEA, Ben-Gurion University of the Negev (BGU), and the Israeli Atomic Energy Commission (IAEC). The main purpose of the campaign was to obtain the core kinetic parameters using various existing and novel noise techniques and compare it with recent measurements. The last time a similar campaign was performed in MINERVE was in 1975 and the core configuration was different (Carre and Oliveira, 1975). This campaign is a continuation of a previous one aimed at determining the delayed neutron fraction β_{eff} in the MINERVE reactor using in-pile oscillations technique (Gilad et al., 2015).

Several well-known and widely used neutron noise techniques were implemented for analyzing the experimental measurements, e.g., power spectral density (PSD, also known as Cohn-α method), Feynman-Y, and Rossi-α methods (Geslot et al., 2015; Perret, 2015). These methods were used to obtain the reactor core's integral kinetic parameters, i.e., the effective delayed neutron fraction β_{eff} and the prompt neutron generation time, including a thorough analysis of the associated uncertainties. More specifically, PSD methods are considered as the standard data processing procedure in the case of a current acquisition system that works at high fission rates by digitizing the current signal issued by fission chambers (Diniz and dos Santos, 2002; dos Santos et al., 2006; Geslot et al., 2015). Such a system has recently been developed and qualified by CEA and is able to process signals on line without any data loss (de Izarra et al.,

* Corresponding author.
E-mail address: gilade@bgu.ac.il (E. Gilad).

http://dx.doi.org/10.1016/j.pnucene.2017.03.019
0149-1970/

2015).

The statistical uncertainties associated with the PSD method are usually thoroughly analyzed and are propagated to the final results, i.e., the integral kinetic parameters, using well established methodologies and considerations. For example, both Geslot et al. (2015) and Perret (2015) recommend using the values obtained by the cross power spectral density (CPSD) estimator following data processing considerations and final uncertainties associated with the results. In their studies, this estimator has proved to be very robust and produced minimum uncertainties. The uncertainties usually considered in the PSD method include statistical fluctuations in the neutron flux, power drifts, uncertainties in the Diven factor, in the integral fission rate, and in the reactivity value. For example, the high-level analysis by Geslot et al. (2015) using PSD techniques leads to uncertainties of 1.8–2.8 pcm in the value of β_{eff} and 0.7–1.3 μs in Λ (at 1σ).

On the other hand, the uncertainty associated with the numerical parameters used in the power spectrum calculation procedure, e.g., the time bin size and the number of points taken in each Fourier transform (buffer size), is hardly discussed in the literature and generally overlooked. Despite their conspicuous importance (as demonstrated in this paper), very little considerations are usually given to their values. These values are often determined rather arbitrarily according to the acquisition system technical specifications and the bias degree of the residuals in the curve fitting procedure. Moreover, well-defined criteria or methodologies for setting and tuning these numerical parameters, as well as for evaluating their associated uncertainties, are generally absent. Examples of numerical parameters used for power spectrum calculations in different studies are given in Table 1.

It should be noted that the precise values of the kinetic parameters are of less importance in this study. Instead, the important result is the methodology for estimation of the propagated uncertainties associated with the numerical parameters and the fact that these are of significant magnitude compared to other uncertainties, thus should not be ignored.

In this paper, the sensitivity of the PSD method to numerical parameters used in the power spectrum calculation is studied by analyzing noise measurements performed in the MINERVE reactor core at three different reactivity states. The associated numerical uncertainties are evaluated and a methodology for optimal determination of these parameters is proposed. The experimental setup is described in section 2, the PSD formalism is introduced in section 3, and the CPSD results for the critical state Acq12 are described and discussed in sections 4. The CPSD results for the subcritical states Acq16 and Acq19 are described in sections 4.3. APSD results for the different reactivity states are described section 4.4 and the conclusions are discussed in section 5.

Table 1
Example of numerical parameters used for power spectrum calculations in different studies.

Reference	Number of points in each Fourier transform	Time bin size [ms]
Kitamura et al. (1999)	–	0.512
Diniz and dos Santos (2002)	800	0.03–2
Diniz and dos Santos (2006)	1600	160
	800	10
dos Santos et al. (2006)	400–800	–
dos Santos et al. (2013)	8192	0.2
Geslot et al. (2015)	2000	1
Perret (2015)	2048	1

2. Experimental setup

The MINERVE reactor is a pool-type ($\sim$120 m^3) reactor operating at a maximum power of 100 W with a corresponding thermal flux of 10^9 n/cm$^2\cdot$s (Bignan et al., 2010). The core is composed of a driver zone, which includes 40 standard highly enriched MTR-type metallic uranium alloy plate assemblies surrounded by a graphite reflector. An experimental cavity, in which various UO_2 or MOX cladded fuel pins can be loaded in different lattices, reproducing various neutron spectra (Bignan et al., 2010; Hudelot et al., 2004), is located in the center of the driver zone. During the experimental campaign, the central experimental zone was loaded with 770 3% enriched UO_2 fuel rods arranged in a lattice representative of a PWR spectrum. An oscillator piston, capable of moving periodically and vertically between two positions located inside and outside of the core is located inside the experimental zone. A general view of the MINERVE reactor is shown in Fig. 1, together with schematic drawings of the reactor geometrical configuration and the MAESTRO core configuration (Leconte et al., 2013).

During the measurement campaign, neutron noise experiments have been conducted in three reactor states; one very close to critical state (marked as “Acq12”) and two different subcritical states (marked as “Acq16” and “Acq19”). The different criticality states were obtained by inserting one of the four control rods into the core. The reactor configuration was that of the MAESTRO program (Leconte et al., 2013), representing a PWR spectrum in the central experimental cavity, as shown in Fig. 1. Two large fission chambers with approximately 1 g of ^{235}U have been installed next to the driver zone (denoted n° 670 and n° 671 in Fig. 1). In order to minimize flux disturbances in the detectors during measurement, reactor criticality was controlled by control rod B1, which is far from the two detectors. During the measurements, the power was regulated by an automatic piloting system that makes use of a low efficiency rotating control rod with cadmium sectors.

The signals were acquired using fast amplifiers and CEA-developed multipurpose acquisition system X-MODE (Geslot et al., 2005). The signals were acquired in time-stamping mode with a resolution of 25 ns. It should be noted that the processed signal was not the digitized, continuous current of a detector. Instead, the number of pulse detections is summed up in time bins to generate a discrete count rate, which is assumed to be proportional to the momentary (sampled) value of the neutron flux.

The only slightly subcritical measurement Acq12 has been conducted at a power of 0.2 W with detectors' count rate around 5.5×10^5 cps. The subcritical measurements Acq16 and Acq19 have been conducted with detectors' count rate around 4×10^4 cps. A count rate sample segment obtained from the detectors' signal is shown in Fig. 2. More details on the experimental setup and acquisition systems can be found in (Geslot et al., 2015; Perret, 2015). The measurements analyzed in this paper are described in Table 2.

3. The power spectral density formalism

The transfer function of the reactor links the neutron noise (statistical fluctuations in the neutron flux around its mean value) to the neutron source fluctuations. The zero power transfer function can be derived from point kinetic equations, where the source noise is considered to be entirely due to fluctuations in the core's reactivity, in the neutron flux and in the precursors concentration (Keepin, 1965; Uhrig, 1970; Williams, 1974). For large enough frequencies, i.e. $\omega \gg \lambda_j$, the square of the amplitude of the zero power transfer function, $|H(\omega)|^2$, can be explicitly expressed in terms of the core's kinetic parameters in the following form (Santamarina et al., 2012)

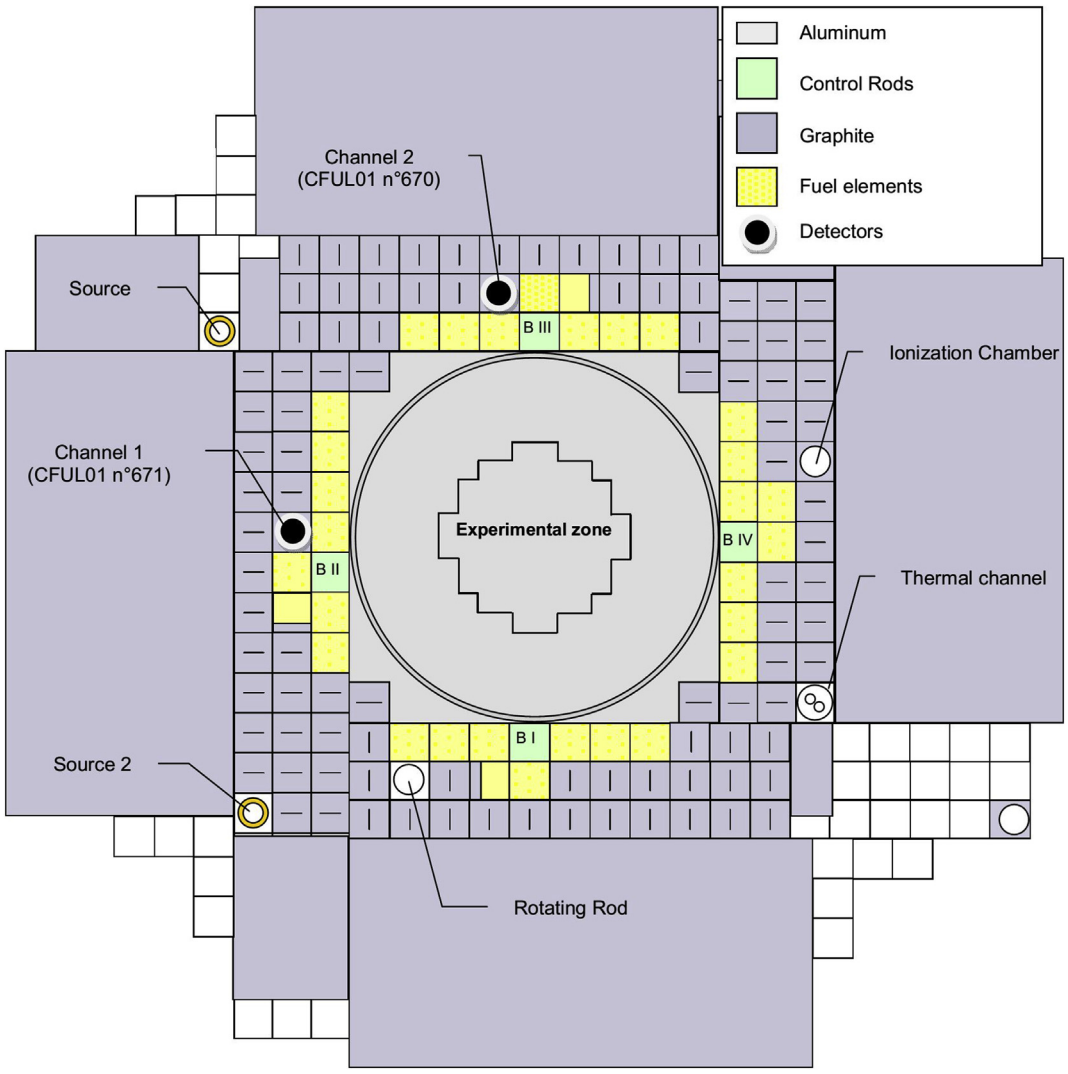

Fig. 1. Schematic layout of the MINERVE zero power reactor core during the noise measurements campaign in Sep. 2014.

$$|H(\omega)|^2 = \frac{\frac{1}{(\beta_{\text{eff}}-\rho)^2}}{1+(\omega/\omega_c)^2}, \tag{1}$$

where β_{eff} is the delayed neutron fraction, ρ is the core's reactivity, $\omega = 2\pi f$ is the angular frequency, and $\omega_c = \frac{\beta_{\text{eff}}-\rho}{\Lambda}$ is called the cutoff frequency. The square of the amplitude of the zero power transfer function can also be written in terms of two detectors' readings $c_1(t)$ and $c_2(t)$ (Cohn, 1960; Uhrig, 1970; Williams, 1974) in the following form

$$|H(\omega)|^2 = \frac{\text{CPSD}(\omega)}{\bar{c}_1\bar{c}_2}\frac{1}{2D/F_0}, \tag{2}$$

where $\bar{c}_i$ is the average count rate of detector i, $D = \frac{\overline{\nu(\nu-1)}}{\bar{\nu}^2}$ is the Diven factor (Diven et al., 1956), F_0 is the integral fission rate in the core, and $\text{CPSD}(\omega)$ is the cross power spectral density of the neutron noise (Uhrig, 1970). Hence, by combining Eqs. (1) and (2), the expression linking the power spectral density of the neutron noise with the core's kinetic parameters is (Cohn, 1960; Carre and Oliveira, 1975; Diniz and dos Santos, 2002; dos Santos et al., 2006)

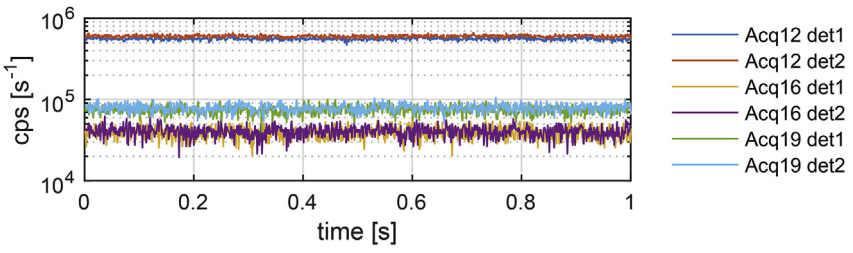

Fig. 2. A sample segment of count rate obtained from the detectors' signals for the different reactivity states.

Table 2
Pile noise measurements during the Sep. 2014 experimental campaign.

Data set	Acq12	Acq16	Acq19
Control rod height [mm]	B1@499	B1@399	B1@449
Core power [W]	0.2	0	0
Duration [s]	5400	5500	5500
Integral fission rate F_0 [s^{-1}]	6.45×10^9	4.00×10^8	7.91×10^8
Reactivity [pcm]	~ 0	-230	-117

$$2\frac{D}{F_0}\frac{\frac{1}{(\beta_{\text{eff}}-\rho)^2}}{1+(\omega/\omega_c)^2}=\frac{\text{CPSD}(\omega)}{\bar{c}_1\bar{c}_2}. \tag{3}$$

Similarly, for the auto power spectral density (APSD), one gets

$$2\frac{D}{F_0}\frac{\frac{1}{(\beta_{\text{eff}}-\rho)^2}}{1+(\omega/\omega_c)^2}=\frac{\text{APSD}_i(\omega)}{\bar{c}_i\bar{c}_i}+B_i, \tag{4}$$

where B_i is some constant due to the fact that unlike CPSD, the APSD does not asymptotically tends to zero due to detections produced by the randomly (uncorrelated) arriving neutrons. For all practical purposes the RHS of Eqs. (3) and (4) is fitted with a function of the form

$$f(\omega)=\frac{x_1}{1+\left(\frac{\omega}{x_2}\right)^2}+x_3 \tag{5}$$

and the kinetic parameters are obtained by

$$\beta_{\text{eff}}-\rho=\sqrt{\frac{2D}{F}\frac{1}{x_1}},\quad \Lambda=\frac{\beta_{\text{eff}}-\rho}{2\pi x_2}. \tag{6}$$

4. Standard PSD analysis

A total of three measurements were analyzed using the PSD method (see Table 2). The Diven factor for thermal fission of ^{235}U is set to $D = 0.8$. The integral fission rate F_0 is obtained by calculation of the flux distribution in the core and its calibration using a dedicated fission chamber located at the center of the core during the experiment. The reactivity worth of the control rod B1 was calculated using rod-drop experiment and inverse kinetics analysis.

The standard PSD procedure usually continues by calculating the power spectral density from the measurement. First, the detector's signal, which is (in this case) a series of time stamps indicating neutron detections in the detector, is binned into consecutive "time bins" of equal size Δt (e.g., Kitamura et al., 1999). The sum of detections in each bin is then divided by the bin size Δt to produce a discrete count rate, denoted by $c_j \equiv c(t_j)$, where $t_j \equiv j\Delta t$. In case of two detectors, denoted by 1 and 2, the corresponding count rates are denoted as $c_{1,j}$ and $c_{2,j}$. Next, the Fourier transform of the series of count rates should be calculated according to the definition of CPSD (Uhrig, 1970)

$$\text{CPSD}(\omega)=\lim_{T\to\infty}\frac{1}{2T}\left[\mathcal{F}_1^*(\omega)\mathcal{F}_2(\omega)\right] \tag{7}$$

where $F_x(\omega)$ is the Fourier transform of the signal from detector x and $F_x^*(\omega)$ stands for its complex conjugate.

In practice, in order to obtain the PSD, a discrete Fourier transform (FFT) is applied to the series of count rates. The Fourier transform is repeatedly applied to consecutive buffers (segments) of the count rate, each of size N. For example, the first spectrum is obtained by applying FFT to the first buffer (i.e., the first N points) $\{c_{1,1},\ldots,c_{1,N}\}$ and $\{c_{2,1},\ldots,c_{2,N}\}$, the second spectrum is obtained by applying FFT to the next buffer $\{c_{1,N+1},\ldots,c_{1,2N}\}$ and $\{c_{2,N+1},\ldots,c_{2,2N}\}$, and so on. The CPSD is obtained by averaging the different spectra and multiply them according to Eq. (7). The time duration of a buffer of size N is denoted by $T = N\Delta t$.

Finally, Eq. (3) is used to obtain $\beta_{\text{eff}} - \rho$ and the cutoff frequency $\omega_c = \frac{\beta_{\text{eff}}-\rho}{\Lambda}$ by Lorentzian curve fitting to the right hand size of the equation. An example for CPSD and APSD for the different reactivity states and a fitted Lorentzian curve are shown in Fig. 3.

Hence, the standard calculation scheme of the PSD inevitably introduces additional purely numerical parameters, *not physical*, into the procedure. These parameters are the time bin size Δt, which is used for the generation of count rates from the time-stamped detector's output and the buffer size N, which is the number of points used for FFT for a single spectrum calculation. Unlike physical parameters of the experimental system, these parameters should have little or no effect on the results of the analysis. For the purpose of this study, the PSD may be viewed as a function of these two parameters in addition to its dependence on the angular frequency, i.e.,

$$\text{PSD}(\omega)\equiv\text{PSD}(\omega;N,\Delta t). \tag{8}$$

In order to evaluate the sensitivity of the calculated kinetic parameters β_{eff} and Λ to these numerical parameters, the calculation procedure is repeated using the same detectors' data but with different numerical parameters. The results for the critical state Acq12 are shown in Fig. 4.

It is clear from Fig. 4 that the numerical parameters N and Δt have a pronounced effect on the obtained kinetic parameters. Initially, no compelling physical arguments favoring a specific set of values for the buffer size N and the time bin size Δt were found. These parameters are usually set such that the sensitivity of the obtained results is minimized and the residuals are normally distributed without any trend at low or high frequencies. Examination of Fig. 4 indeed reveals areas in the numerical parameters' space where the value of β_{eff} is only weakly sensitive to the parameters values, but no such areas are found for Λ.

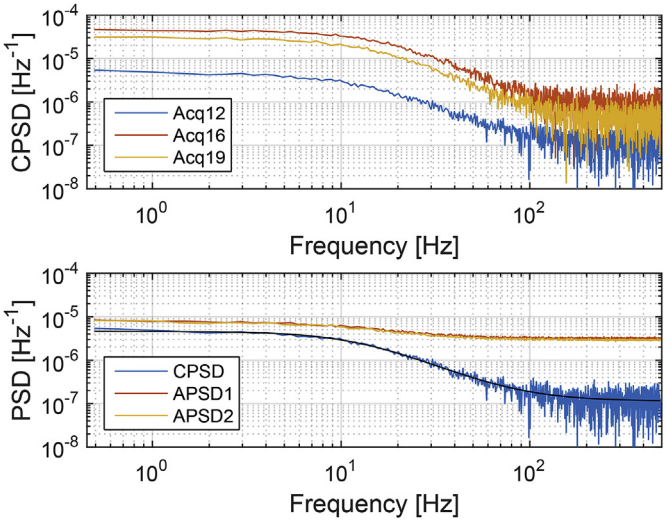

Fig. 3. Upper panel: An example of CPSD for the different reactivity states. Lower panel: An example of APSD and CPSD for Acq12 and the fitted Lorentzian curve (marked by solid black line). The PSDs were calculated using time bin size $\Delta t = 1.02$ ms and buffer size $N = 2000$ points.

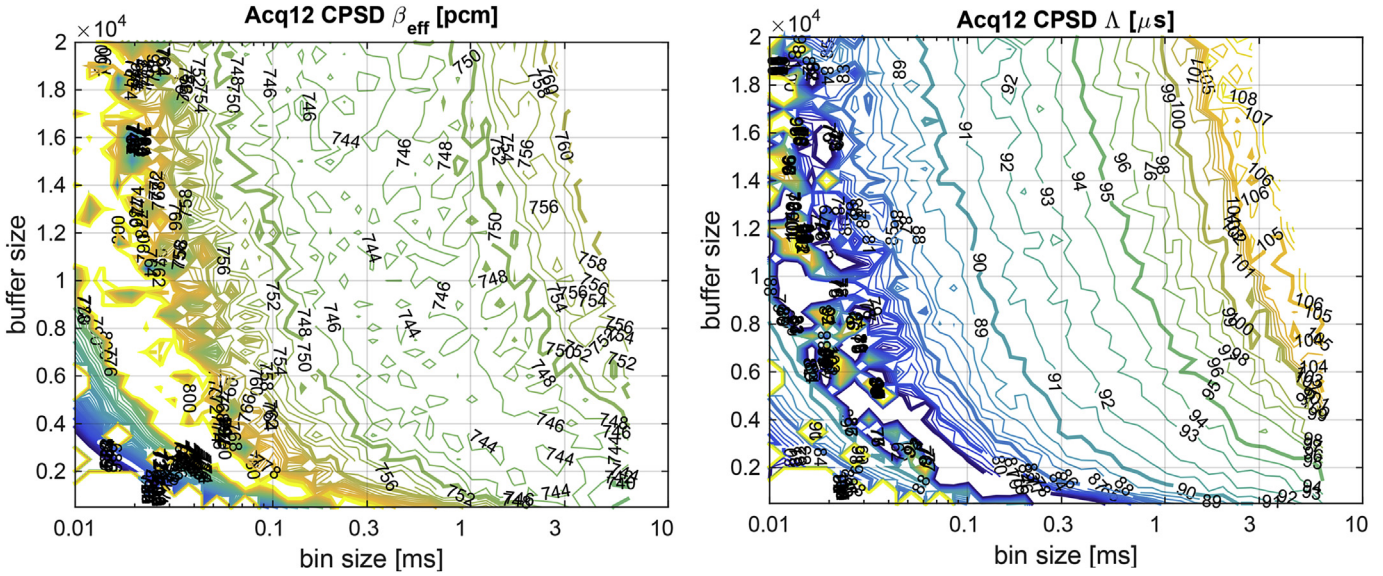

Fig. 4. Sensitivity of the obtained effective delayed neutron fraction β_{eff} and the prompt neutron generation time Λ to the buffer size N and the time bin size Δt for the critical state Acq12 using CPSD method.

4.1. The relevant frequency range

The irregular and erratic behavior of the fit results in the left and lower left parts of the parameter space (mainly small Δt) is due to the fact that the relevant frequency range, where the PSD possesses physical meaning (and is not white noise), is roughly between 1 and 80 Hz (Geslot et al., 2015; Perret, 2015). This range depends of course on the physical properties of the specific core and can assume different values. Moreover, the kinetic parameters presented in Fig. 4 are fitted over the entire spectrum and not confined to some predefined frequency range.

Let us define an "appropriate" spectrum as a spectrum that can be used for curve fitting in the frequency range 1–80 Hz and therefor can be used for calculation of the kinetic parameters. Such a spectrum needs to contains the frequency range 1–80 Hz, i.e., its minimal frequency should be less than 1 Hz and its maximal frequency (the Nyquist frequency) should be larger than 80 Hz. These two extreme frequencies are solely and uniquely determined by the buffer size N and the time bin size Δt. The Nyquist frequency is defined according to

$$f_{max} = \frac{1}{2\Delta t} \tag{9}$$

and the minimal frequency, which is equivalent to the spectrum resolution, is determined according to

$$f_{min} = \Delta f = \frac{1}{T} = \frac{1}{N\Delta t}. \tag{10}$$

According to the above definition of an "appropriate" spectrum, one can define an "appropriate" set of numerical parameters $(\Delta t, N)$ using Eqs. (9) and (10). The requirement $f_{max} \geq 80$ Hz imposes an upper limit on the time bin size, i.e., $\Delta t \leq 6.25$ ms. The requirement $f_{min} \leq 1$ Hz implies that $N\Delta t \geq 1$ s. The values of f_{min} as a function of Δt and N are illustrated in Fig. 5, where the line $\Delta t = 6.25$ ms is also marked. Thus, any pair $(\Delta t, N)$ that fulfills these requirements (i.e., define a frequency range for the spectrum that includes the range 1–80 Hz) can be used for PSD fit procedure.

Points A-E in Fig. 5 represent appropriate pairs $(\Delta t, N)$ for PSD fit, i.e., the PSD range includes the 1–80 Hz range. Point F represent inappropriate pair for PSD fit. The parameters of points A-F are given in Table 3 and the corresponding spectra and Lorentzian fits are shown in Fig. 6.

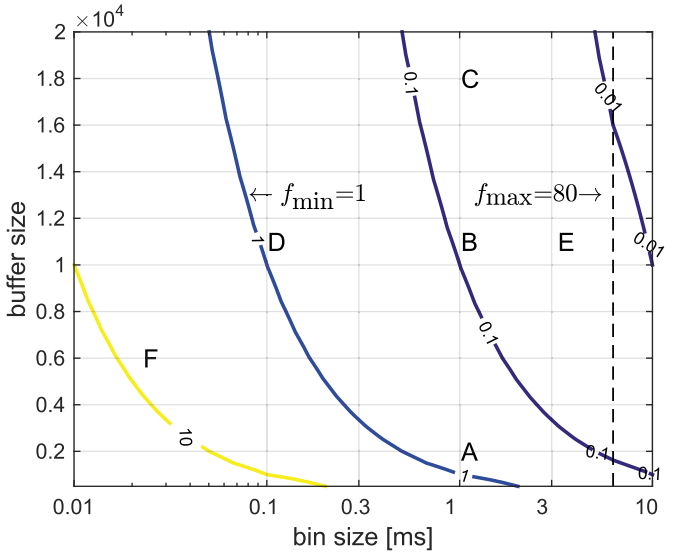

Fig. 5. The values of f_{min} and f_{max} as a function of Δt and N. The line $\Delta t = 6.25$ ms is marked with dashed black line. Points A-E represent "appropriate" sets of values $(\Delta t, N)$. Point F represent "inappropriate" set of values for PSD fit.

Table 3
Parameters of points A-F in Fig. 5.

Point	Δt [ms]	N	$f_{min} - f_{max}$ [Hz]	β_{eff} [pcm]	Λ [μs]
A	1.02	2000	0.49–492	744	91
B	1.02	11000	0.09–492	747	97
C	1.02	18000	0.05–492	750	99
D	0.10	11000	0.90–4960	751	90
E	3.23	11000	0.03–155	755	105
F	0.02	6000	7.30–21900	869	106

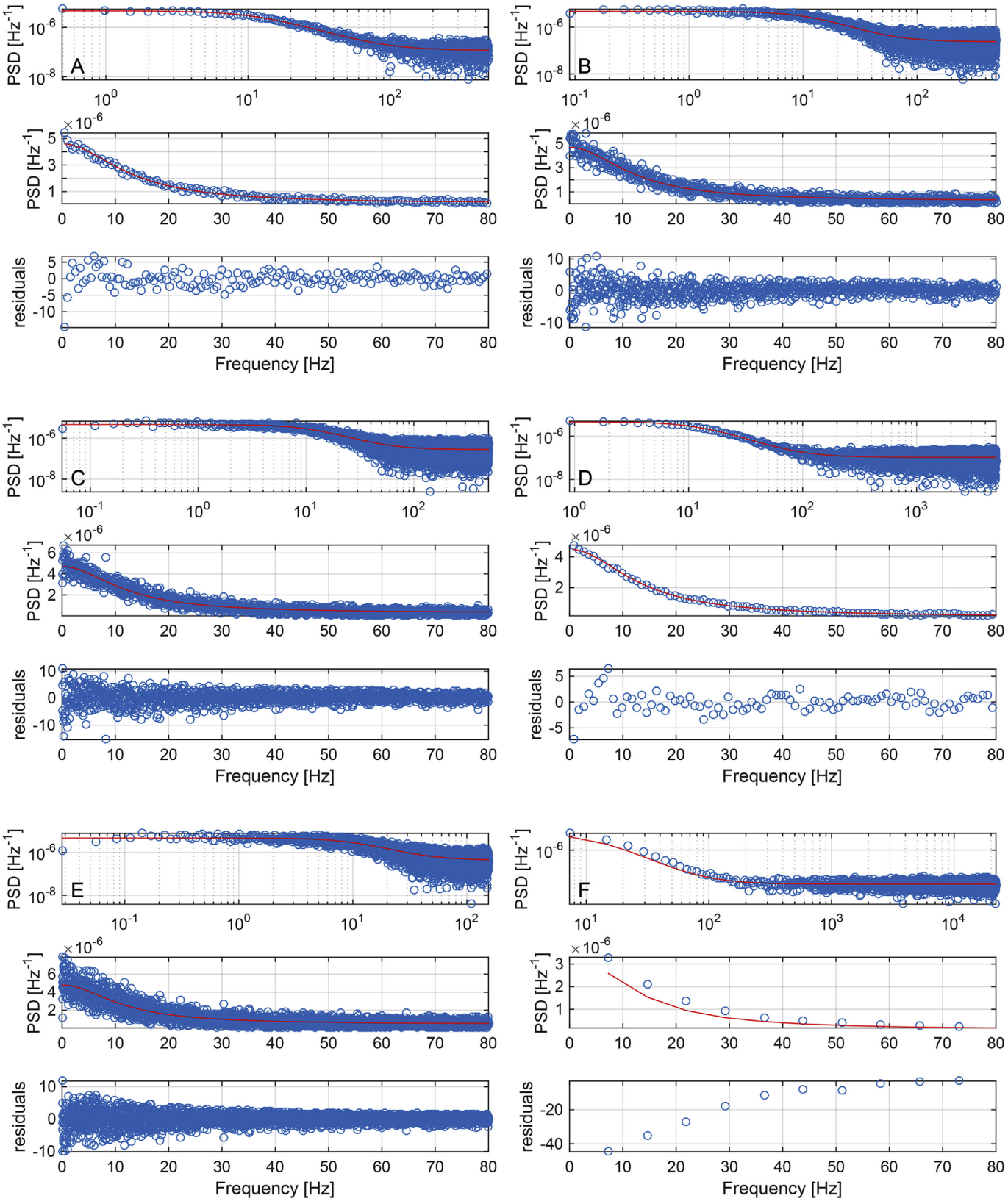

Fig. 6. Full spectra (upper panel), Lorentzian fit on the range 1–80 Hz (middle panel), and the normalized residuals (lower panel) for the points A-F detailed in Table 3 and shown in Fig. 5.

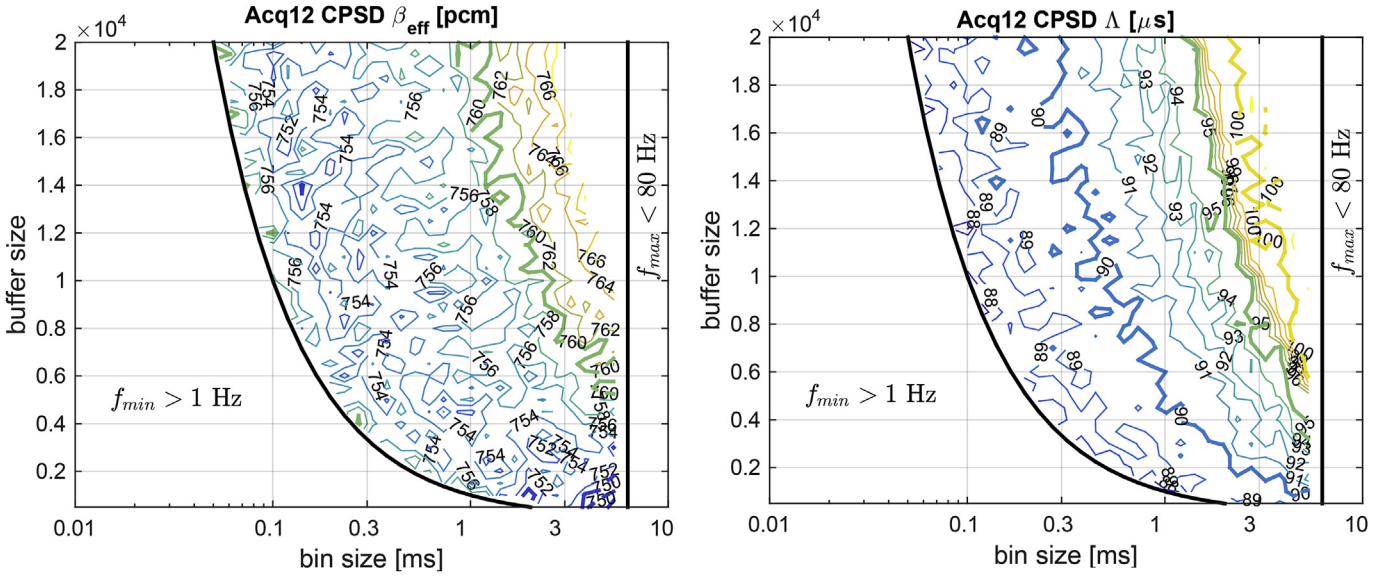

Fig. 7. Sensitivity of the obtained kinetic parameters to the buffer size N and the time bin size Δt over the relevant frequency range for the critical state Acq12 using CPSD.

The striking observation from Fig. 6 and Table 3 is that all points A-E cover very well the relevant section of the transfer function, i.e., the relevant bandwidth 1–80 Hz, and they all exhibit excellent fits with uniform distribution of the normalized residuals. Hence, all these point are appropriate for PSD analysis and derivation of the kinetic parameters. However, as shown in Table 3, the obtained values of the kinetic parameters vary significantly between the different points, where no point is favored over the other.

Once we have established some guide rules for selecting appropriate pairs of $(\Delta t, N)$ values, Fig. 4 is redrawn in Fig. 7 only for appropriate parameters which enable proper fit procedure. This representation of the sensitivity of the obtained kinetic parameters is much more insightful since although any point in Fig. 7 is legitimate for the Lorentzian fit procedure, the variance in the obtained results is significant. For example, Geslot et al. (2015) calculated the PSD using $\Delta t = 1$ ms and $N = 2000$. Looking at Fig. 7, this point is part of a large set of equivalent points where none are physically favored, but produce different results.

Two points are worth mentioning. First, aliasing errors are negligible in this case since for most time bins the Nyquist frequency is much larger than twice the cutoff frequency, which is 80 Hz (the upper limit for Lorentzian fit). The only spectra which may be affected by aliasing are those corresponding to $\Delta t \gtrsim 5$ ms. Numerical tests reveal that the fit results in this region are not affected even for 50% removal of the higher spectrum. Second, the DC component of each spectrum is removed, thus ensuring the signals are characterized by zero mean.

4.2. Quantifying the uncertainty

One possible course of action in determining the values of β_{eff} and Λ is to average their values over the appropriate set of $(\Delta t, N)$ values according to Fig. 7. Appropriate pairs of $(\Delta t, N)$ ensure relevant frequency range for fit and they are all physically equivalent. The standard deviation over this appropriate set can be used as a measure of the propagated uncertainties associated with the choice of numerical parameters such as Δt and N. In the case of CPSD analysis of the critical state Acq12 shown in Fig. 7, the mean and standard deviation are $\beta_{\text{eff}} = 756.7 \pm 3.8$ pcm and $\Lambda = 91.7 \pm 3.6$ μs.

4.3. CPSD results for subcritical states

The CPSD analysis described in section 4 was also applied to the two subcritical states Acq16 and Acq19. The results are shown in Fig. 8 and exhibit similar qualitative and quantitative behavior of the kinetic parameters' sensitivity to the choice of numerical parameters Δt and N. The means and standard deviations over the appropriate set of numerical parameters are $\beta_{\text{eff}} = 734.4 \pm 4.4$ pcm and $\Lambda = 91.6 \pm 3.0$ μs for Acq16 and $\beta_{\text{eff}} = 715.4 \pm 3.1$ pcm and $\Lambda = 89.6 \pm 3.2$ μs for Acq19.

Moreover, comparing to Fig. 7, it seems that the sensitivity of the CPSD and the kinetic parameters in subcritical states exhibit smoother and more homogeneous behavior over the parameter space with respect to the critical state. This could be related to the fact that the statistical errors associated with higher moments of the count rate (used in estimators like CPSD, APSD, Fyenman-α, etc.) converge faster for subcritical measurements than for critical ones. As a general rule, the convergence rate of the variance of higher moments is proportional to the inverse of the reactivity. More specifically, the statistical variance of moment M_n of order n converges at a rate inversely proportional to the reactivity to the power of $2n$, i.e., $Var(M_n) \sim \frac{1}{\rho^{2n}}$ (Dubi and Kolin, 2016).

4.4. APSD results

An APSD analysis was carried out on all three reactivity states along the guidelines that were phrased in section 4 regarding the appropriate set of numerical parameters to be used for fit procedure. The sensitivity of the obtained kinetic parameters to the choice of Δt and N exhibits similar qualitative behavior as exhibited in the CPSD analysis. An example is shown in Fig. 9 for both APSD_1 and APSD_2 analysis of the critical state Acq12.

Qualitatively, the sensitivity of the kinetic parameters to the numerical parameters obtained via APSD analyses for both subcritical states, Ac16 and Acq19, exhibit very similar behavior to the one showed in Fig. 9, although quantitatively the APSD analyses produce different results for β_{eff} and Λ. The results of both CPSD and APSD analyses of all three reactivity states, including the mean values and standard deviations are summarized in Table 4. It should be noted that the uncertainties presented in Table 4 under the "Current work" column are associated ***only*** with the numerical

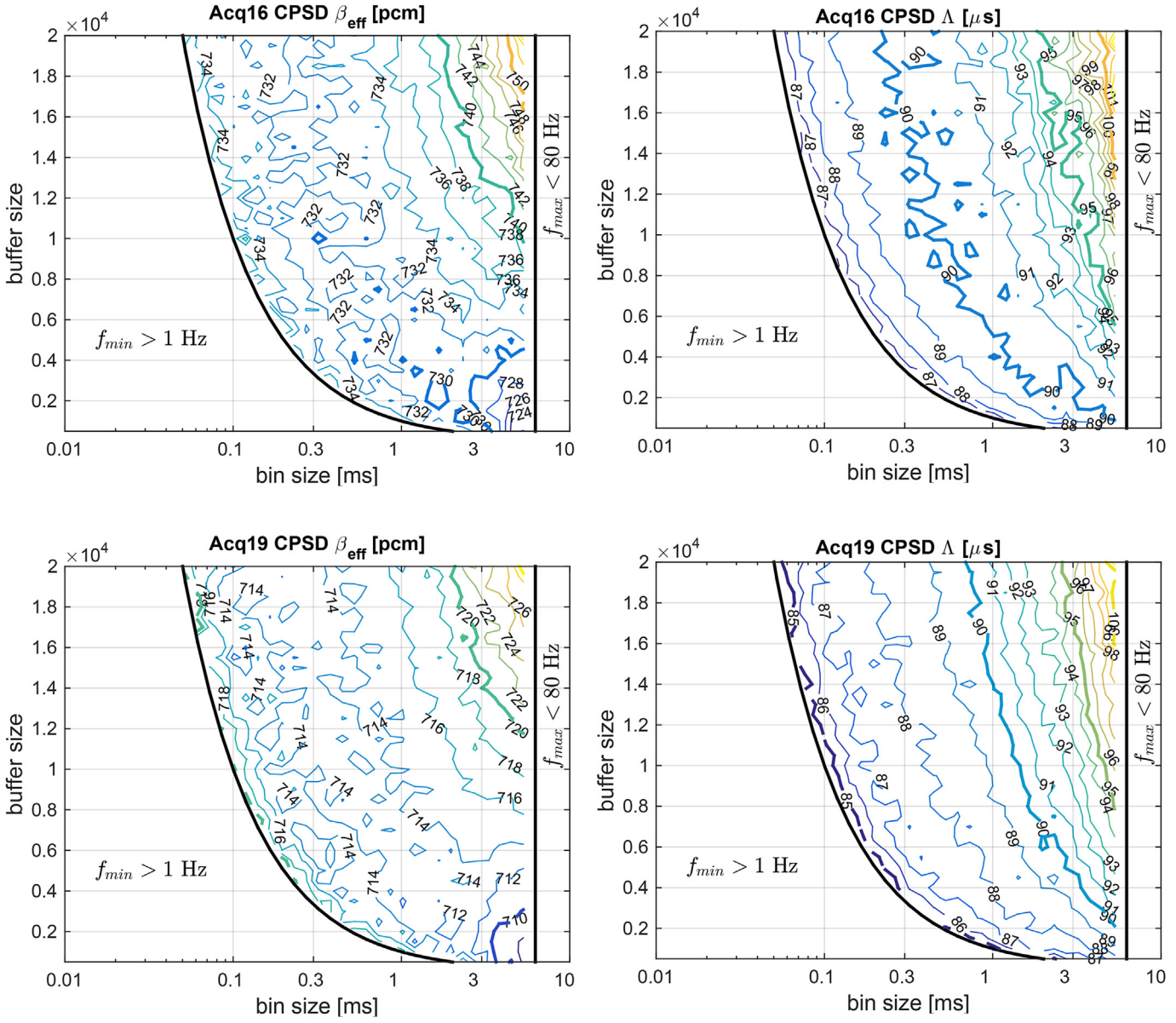

Fig. 8. Sensitivity of the obtained kinetic parameters to the buffer size N and the time bin size Δt over the appropriate set of numerical parameters for the subcritical states Acq16 and Acq19 using CPSD analysis.

parameters Δt and N disregarding any other sources of uncertainty.

The discrepancies in the results are two fold. First, the CPSD and the APSD results are in well agreement for the critical state Acq12, and also agree well with the results obtained by Geslot et al. (2015) for β_{eff} (but less for Λ). However, the discrepancies between the results associated separately with each detector, i.e., APSD_1 and APSD_2, increase as the core becomes more subcritical. Generally, results obtained using counts from detector 1 clearly exceed the results obtained using counts from detector 2 for both β_{eff} and Λ. This disagreement was also observed by Gilad et al. (2016), where the subcritical states were analyzed using a completely different method, i.e., the Feynman-Y method. Second, it seems that the subcriticality level of the core during the experiment significantly influences the results and neither the CPSD nor the APSD methods produce consistent results for the kinetic parameters by analyzing the different reactivity states.

Several possible sources for the dispersion of the results from the two detectors comes to mind. The detection efficiency is different between the two detectors, which lead to small discrepancies between the statistical characteristics of their associated neutron counts. Although these discrepancies are small, the fact that no dead-time correction was applied to any of the detectors' counts may increase the observed inconsistency (the CPSD is somewhat less sensitive to dead-time corrections than APSD). Moreover, different geometrical positions of the detectors may give rise to small spatial effects. Finally, inconsistencies in the evaluation of the subcriticality levels of the different states (as suggested by Gilad et al., 2016) or in the evaluation of the integral fission rates can inflict significant deviations on the obtained kinetic parameters.

The dispersion of the results is important, real, and no obvious trend can be identified, which makes the use of average results a bit

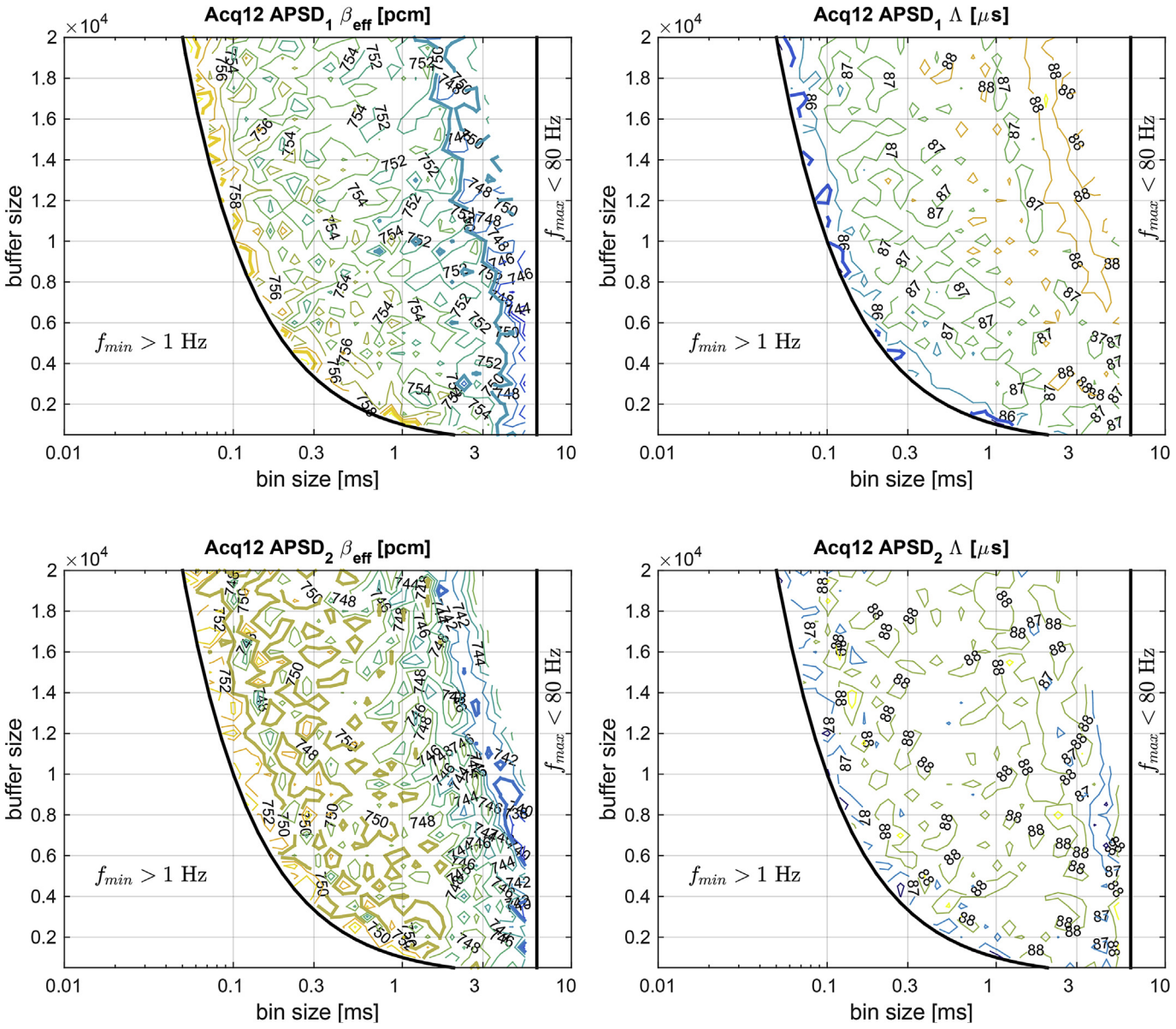

Fig. 9. Sensitivity of the obtained kinetic parameters to the buffer size N and the time bin size Δt over the appropriate set of numerical parameters for the critical state Acq12 using $APSD_1$ (upper panels) and $APSD_2$ (lower panels) analysis.

unreliable. Having said that, a thorough analysis of these discrepancies is beyond the scope of this paper and will be published elsewhere. This paper focuses more on the uncertainties associated with numerical parameters of the PSD techniques and less with the absolute values of the obtained kinetic parameters.

5. Discussion and conclusions

Standard uncertainty analysis of PSD techniques usually considers important sources for uncertainty, e.g., statistical fluctuations in the neutron count, power drifts, uncertainties in the Diven factor, in the integral fission rate, and in the reactivity value. These uncertainties are then propagated through the PSD procedure in order to evaluate the total uncertainties in the obtained kinetic parameters. For example, the analysis by Geslot et al. (2015) on the same data for the critical state using PSD techniques leads to uncertainties of 1.8–2.8 pcm in the value of β_{eff} and 0.7–1.3 μs in Λ (at 1σ).

However, the uncertainty associated with the numerical parameters used in the power spectrum calculation procedure, e.g., time bin size Δt and buffer size N, is hardly discussed in the literature and generally overlooked, whereas these parameters are often determined rather arbitrarily according to the acquisition system technical specifications. Moreover, well-defined criteria or methodologies for evaluating their associated uncertainties are not addressed.

In this paper, the PSD method is implemented to analyze critical and subcritical configurations of the MAESTRO core in the MINERVE zero power reactor in order to measure its integral kinetic parameters, i.e. effective delayed neutron fraction β_{eff} and the prompt neutron generation time Λ.

The sensitivity of the obtained kinetic parameters to the choice of numerical parameters used for spectrum calculations is studied and found to be pronounced. Examination of this sensitivity (Fig. 4)

Table 4
Mean and standard deviation (1σ) of the obtained kinetic parameters over the appropriate set of numerical parameters for both CPSD and APSD analyses of three reactivity states. The emphasized values are the mean and RMS of the different CPSD/APSD results. The uncertainties presented under the "Current work" column are associated *only* with the numerical parameters Δt and N, disregarding any other sources of uncertainty.

Reactivity state	PSD method	Current work		Geslot et al. (2015)	
		β_{eff} [pcm]	Λ [μs]	β_{eff} [pcm]	Λ [μs]
Acq12	CPSD	756.7±3.8	91.7±3.6	746.8±1.8	94.5±0.7
	$APSD_1$	753.2±3.3	87.1±0.8	750.4±2.8	94.8±1.3
	$APSD_2$	748.0±3.7	87.7±0.6	749.1±2.4	93.7±1.1
		752.6±3.6	**88.8±2.2**	**748.8±2.4**	**94.3±1.1**
Acq16	CPSD	734.4±4.4	91.6±3.0	–	–
	$APSD_1$	769.0±4.9	93.4±1.3	–	–
	$APSD_2$	683.6±4.4	86.8±0.9	–	–
		729.0±4.6	**90.4±2.0**	–	–
Acq19	CPSD	715.4±3.1	89.6±3.2	–	–
	$APSD_1$	724.5±3.2	89.1±1.0	–	–
	$APSD_2$	694.3±2.8	84.0±0.9	–	–
		711.4±3.0	**87.6±2.0**	–	–

reveals extremely sensitive and erratic behavior of the fit results for small Δt and a wide range of N values, due to inappropriate frequency range for the PSD, i.e., the PSD does not contain the physically relevant frequency range of the zero power transfer function, which is estimated roughly to be between 1 and 80 Hz for the MAESTRO core configuration.

This extremely sensitive and erratic behavior is eliminated once the numerical parameter space $(\Delta t, N)$ is restricted to appropriate values, which define an appropriate frequency range for the PSD. However, although the sensitivity of the obtained kinetic parameters to the numerical parameters is reduced dramatically, it does not become negligible and show pronounce changes over the $(\Delta t, N)$ space (Figs. 7–9).

Essentially, the different PSDs, which are derived from the same measured data (e.g., Acq12, Acq16, or Acq19) using different sets of numerical parameters $(\Delta t, N)$, encapsulate the same amount of information. The different choices of numerical parameters simply distribute this information (i.e., PSD) differently in the frequency domain. Larger buffer size N (larger number of points included in each FFT) leads to finer resolution in the frequency domain but less statistics on each point, whereas small buffer size leads to coarser spectral resolution but better statistics on each point. This trade-off behavior affects the fit procedure, as nicely demonstrated by considering points A (small buffer size) and C (large buffer size) in Figs. 5 and 6.

It should be noted that the choice to fit the Lorentzian curve using PSD in the range 1–80 Hz, although based on physical considerations, is rather arbitrary and this arbitrariness is inflicted on the uncertainty. This frequency range should be set according to the form of the reactor's transfer function and the signal-to-noise ratio. The sensitivity of the obtained kinetic parameters to the fitting range was superficially examined by using the range 1–120 Hz for comparison, which yielded no significant differences.

A novel methodology is proposed for analyzing the kinetic parameters' sensitivity to the PSD and for quantifying the associated uncertainty. Since any point in the numerical parameter space that satisfies the requirements for physically interesting frequency range (Fig. 5) is adequate for Lorentzian fit, it is suggested that the values of the kinetic parameters and the associated uncertainties may be determined by the mean and standard deviation of these parameters over the appropriate numerical parameter space. It should be noted that the fit results exhibit rather smooth and robust behavior over the numerical parameter space.

The uncertainties originate from the sensitivity of the kinetic parameters to the numerical parameters used for PSD calculation are summarized in Table 4. The uncertainty value for the critical state (Acq12) in β_{eff} is 3.8 pcm for CPSD and $\sim$ 3.5 pcm for APSD analyses, and in Λ is 3.6 μs for CPSD and $\sim$ 0.7 μs for APSD analyses. These values are significant and non-negligible comparing to the corresponding 1.8–2.8 pcm and 0.7–1.3 μs uncertainty values calculated by Geslot et al. (2015) (which do not consider the numerical uncertainty), where the PSD was calculated at a single point in the $(\Delta t, N)$ space, i.e., $\Delta t = 1$ ms and $N = 2000$.

The discrepancies between the results associated separately with each detector increase as the core becomes more subcritical and results obtained using counts from detector 1 clearly exceed the results obtained using counts from detector 2 for both β_{eff} and Λ. This disagreement was also observed by Gilad et al. (2016), where the subcritical states were analyzed using the Feynman-Y method, which is different from PSD methods in that it is not based on the reactor transfer function. Several possible sources for the dispersion of the results from the two detectors are discussed in section 4.4, e.g. the absence of dead-time correction, spatial effects, inconsistencies in the evaluation of the subcriticality levels and in the evaluation of the integral fission rates. Although the dispersion of the results is important, a thorough analysis of these discrepancies is beyond the scope of this paper.

We conclude by stating that the uncertainties in the kinetic parameters (β_{eff} and Λ) calculated using PSD methods, which are associated with the numerical parameters time bin size Δt and buffer size N, used for spectrum calculations, are significant and should not be neglected.

References

Bignan, G., Fougeras, P., Blaise, P., Hudelot, J.-P., Mellier, F., 2010. Reactor Physics Experiments on Zero Power Reactors, vol. III. Springer, pp. 2084–2096. Ch. 18.

Carre, J., Oliveira, J.D.C., 1975. Measurements of kinetic parameters by noise techniques on the MINERVE reactor. Ann. Nucl. Energy 2 (2), 197–206.

Cohn, C.E., 1960. A simplified theory of pile noise. Nucl. Sci. Eng. 7, 472–475.

de Izarra, G., Jammes, C., Geslot, B., Di Salvo, J., Destouches, C., 2015. SPECTRON, a neutron noise measurement system in frequency domain. Rev. Sci. Instrum. 86 (11), 115111. http://scitation.aip.org/content/aip/journal/rsi/86/11/10.1063/1.4935250.

Diniz, R., dos Santos, A., 2002. A noise analysis approach for measuring the decay constants and the relative abundance of delayed neutrons in a zero power critical facility. J. Nucl. Sci. Technol. (Sup. 2), 669–672.

Diniz, R., dos Santos, A., 2006. Experimental determination of the decay constants and abundances of delayed neutrons by means of reactor noise analysis. Nucl. Sci. Eng. 152, 125–142.

Diven, B.C., Martin, H.C., Taschek, R.F., Terrell, J., 1956. Multiplicities of fission neutrons. Phys. Rev. 101, 1012–1015.

dos Santos, A., Diniz, R., Fanaro, L.C., Jerez, R., de Andrade e Silva, G.S., Yamaguchi, M., 2006. A proposal of a benchmark for beff, beff/l, and l of thermal reactors fueled with slightly enriched uranium. Ann. Nucl. Energy 33 (9), 848–855. http://www.sciencedirect.com/science/article/pii/S0306454906000600.

dos Santos, A., Lee, S.M., Diniz, R., Jerez, R., 2013. A new experimental approach for subcritical reactivity determination of multiplying systems. Ann. Nucl. Energy 59, 243–254. http://www.sciencedirect.com/science/article/pii/S030645491300217X.

Dubi, C., Kolin, A., 2016. Analytic derivation of the statistical error in the Feynman-method. Ann. Nucl. Energy 88, 186–193. http://www.sciencedirect.com/science/article/pii/S0306454915005277.

Geslot, B., Gruel, A., Pepino, A., Salvo, J.D., de Izarra, G., Jammes, C., Destouches, C., Blaise, P., 2015. Pile noise experiment in MINERVE reactor to estimate kinetic parameters using various data processing methods. In: 4th ANIMMA, 20–24 April 2015, Lisbon.

Geslot, B., Jammes, C., Nolibe, G., Fougeras, P., May 2005. Multimode acquisition system dedicated to experimental neutronic physics. In: 2005 IEEE Instrumentationand Measurement Technology Conference Proceedings, vol. 2, pp. 1465–1470.

Gilad, E., Kolin, A., Rivin, O., Dubi, C., Geslot, B., Blaise, P., 2016. Analysis of critical and subcritical neutron noise experiments in MINERVE using advanced noise techniques. In: PHYSOR 2016: Unifying Theory and Experiments in the 21st Century. May 1-5, 2016, Sun Valley, Idaho, USA.

Gilad, E., Rivin, O., Ettedgui, H., Yaar, I., Geslot, B., Pepino, A., Salvo, J.D., Gruel, A., Blaise, P., 2015. Experimental estimation of the delayed neutron fraction of the

MAESTRO core in the MINERVE zero power reactor. J. Nucl. Sci. Technol. 52 (7–8), 1026–1033.
Hudelot, J.P., Klann, R., Fougeras, P., Jorion, F., Drin, N., Donnet, L., 2004. OSMOSE: an experimental program for the qualification of integral cross sections of actinides. In: PHYSOR 2004. Illinois, Chicago. April 25–29.
Keepin, G.R., 1965. Physics of Nuclear Kinetics. Addison-Wesley.
Kitamura, Y., Matoba, M., Misawa, T., Unesaki, H., Shiroya, S., 1999. Reactor noise experiments by using acquisition system for time series data of pulse train. J. Nucl. Sci. Technol. 36 (8), 653–660.
Leconte, P., Geslot, B., Gruel, A., Pepino, A., Derriennic, M., Di-Salvo, J., Antony, M., Eschbach, R., Cathalau, S., 2013. MAESTRO: an ambitious experimental programme for the improvement of nuclear data of structural, detection, moderating and absorbing materials - first results for nat V, 55Mn, 59Co and 103Rh. In: 3rd ANIMMA, 23–27 June 2013, Marseille, France.
Perret, G., 2015. Delayed neutron fraction and prompt decay constant measurement in the MINERVE reactor using the PSI instrumentation. In: 4th ANIMMA, 20–24 April 2015, Lisbon.
Santamarina, A., Blaise, P., Erradi, L., Fougeras, P., 2012. Calculation of LWR beff kinetic parameters: validation on the MISTRAL experimental program. Ann. Nucl. Energy 48, 51–59.
Uhrig, R.E., 1970. Random Noise Techniques in Nuclear Reactor Systems. Ronald Press Company.
Williams, M.M.R., 1974. Random Processes in Nuclear Reactors. Pergamon Press.